The Journal of Chemical Physics

Excitation energies, photoionization cross sections, and asymmetry parameters of the methyl and silyl radicals

Cite as: J. Chem. Phys. **141**, 074308 (2014); https://doi.org/10.1063/1.4892584
Submitted: 27 May 2014 . Accepted: 28 July 2014 . Published Online: 18 August 2014

A. M. Velasco, C. Lavín, O. Dolgounitcheva, and J. V. Ortiz

AIP Publishing

Excitation energies, photoionization cross sections, and asymmetry parameters of the methyl and silyl radicals

A. M. Velasco,[1] C. Lavín,[1,a)] O. Dolgounitcheva,[2] and J. V. Ortiz[2]
[1]*Departmento de Química Física, Universidad de Valladolid, 47005 Valladolid, Spain*
[2]*Department of Chemistry and Biochemistry, Auburn University, Auburn, Alabama 36849-5312, USA*

(Received 27 May 2014; accepted 28 July 2014; published online 18 August 2014)

Vertical excitation energies of the methyl and silyl radicals were inferred from *ab initio* electron propagator calculations on the electron affinities of CH_3^+ and SiH_3^+. Photoionization cross sections and angular distribution of photoelectrons for the outermost orbitals of both CH_3 and SiH_3 radicals have been obtained with the Molecular Quantum Defect Orbital method. The individual ionization cross sections corresponding to the Rydberg channels to which the excitation of the ground state's outermost electron gives rise are reported. Despite the relevance of methyl radical in atmospheric chemistry and combustion processes, only data for the photon energy range of 10–11 eV seem to be available. Good agreement has been found with experiment for photoionization cross section of this radical. To our knowledge, predictions of the above mentioned photoionization parameters on silyl radical are made here for the first time, and we are not aware of any reported experimental measurements. An analysis of our results reveals the presence of a Cooper minimum in the photoionization of the silyl radical. The adequacy of the two theoretical procedures employed in the present work is discussed. [http://dx.doi.org/10.1063/1.4892584]

I. INTRODUCTION

Free radicals are molecular species of great importance as intermediates in the mechanisms of many reactions that take place in the atmosphere and in various astronomical objects. In addition, radicals play an important role in the deposition processes in molecular plasmas.[1] CH_3 and SiH_3 are typical examples of free radicals. These radicals are relevant in different contexts. The methyl radical is one of the best characterized transient polyatomic radicals in combustion and in tropospheric chemistry. CH_3 is an important intermediate in hydrocarbon plasmas and in the atmospheric oxidation of many organic species.[2] Methyl radical has also been detected in the interstellar clouds,[3] and in the upper atmospheres of Saturn[4] and Neptune,[5] where it is one of the main products of methane photolysis. The silyl radical, which is isovalent with the methyl radical, is probably the most important transient radical containing second-row elements.[6] It is an intermediate in silane-discharge plasma and it has been reported to play an important role in chemical vapor deposition processes of silicon-containing thin-films from silane.[7]

Molecular photoionization processes play an important role in atmospheric chemistry, astrophysics and industrial plasma. For instance, the photochemical models of the atmosphere of Titan, the largest moon of Saturn, have to include branching ratios of the radicals formed in the methane photolysis products.[8] Photoionization cross sections of these radicals are necessary to convert mass spectrometry investigations of the photofragments into quantified branching ratios. Measurements of photoionization cross sections of molecules and radicals are also necessary to use photoionization mass spectrometric experiments in chemical kinetics or combustion studies.[2,9] Absolute photoionization cross sections of reactive radicals are far less well-known than those of stable molecules. The ephemeral nature of radicals is chiefly responsible for making their detection difficult.[10] Experimental measurements concerning photoionization cross section of methyl and silyl radicals are difficult to perform, for the absolute concentration of radicals is difficult to measure.

Given that methyl radical plays a key role in hydrocarbon photochemistry, investigation of properties related to its spectrum has attracted much attention. Several theoretical and experimental works on the CH_3 radical can be found in the literature that focus chiefly on the discrete spectral region. Studies of the continuum spectral region of this important radical appear to be scarce at the experimental level and non-existent theoretically, as far as it looked to us. The first measurements on photoionization cross-sections of methyl radical were done recently by Taatjes[2] in the photon energy range of 10.2–11 eV. Later, Gans *et al.*[8] measured the absolute photoionization cross sections of methyl radical CH_3 between its ionization threshold and 11.5 eV. These authors have claimed that an accurate knowledge of the photoionization cross section for this and other small hydrocarbon radicals is necessary for understanding the photochemistry of planetary and cometary atmospheres. Much less spectroscopic investigation has been made of silyl radical, even though it is an important intermediate in the mechanism of the gas-phase chemical transformations of silicon molecules.[11] In fact, to the best of our knowledge, photoionization cross sections of SiH_3 have not been reported to date.

Motivated by the general interest in radicals, we have undertaken the theoretical study of some relevant spectral

a)Author to whom correspondence should be addressed. Electronic mail: clavin@qf.uva.es

features of the methyl and silyl radicals. The ultraviolet absorption spectra of both radicals consist mainly of bands associated with excitations from the outermost electron in the ground state to Rydberg states.[12–16] In this work, we have determined excitation energies of a number of Rydberg states of CH_3 and SiH_3 by using electron propagator methods.[17–19] Vertical electron affinities of the corresponding, closed-shell cations have been calculated with several electron-propagator approximations and basis sets with many diffuse functions that are capable of describing the Rydberg states of the radicals. Excitation energies of the radicals may be inferred from differences between the electron affinities.

As reported above, photoionization cross section measurements in methyl radical are limited to photon energies of a few eV above the ionization threshold despite the need in modeling studies for cross sections for photoionization processes over wide spectral regions.[20] Hence, one of the main goals of the present study is to provide the photoionization cross section profile for the outermost orbital of methyl radical over a more extended photon energy range (up to 50 eV). It is also the purpose of this work to predict photoionization cross sections for silyl radical which might be of help in future experimental investigations on this radical.

In earlier works[21,22] the molecular quantum defect orbital (MQDO) method has been used for the study of the discrete spectra of both methyl and silyl radicals. This approach has proved to be reliable in photoionization studies on radicals such as NO, CH, NH_4, and H_3O.[23–25] Here, we have calculated photoionization cross section for the production of the CH_3^+ and SiH_3^+ ions in their lower electronic states with the MQDO method. In addition, we have analyzed the contribution of the different Rydberg series that constitute the ionization channels from the outermost orbitals for both radicals. We have also determined the photoelectron asymmetry parameters as a function of photoelectron energy for the ionization of the outermost valence orbitals of the methyl and silyl radicals. In recent applications to molecules containing first-row elements,[26,27] the comparison of the MQDO asymmetry parameters with experimental results showed the reliability of the computational method. The present calculations predict a Cooper minimum in the asymmetry parameter profile of the silyl radical. Further investigations are desirable to confirm the presence of a Cooper minimum in the photoionization of SiH_3.

II. METHODS OF CALCULATION

A. Electron propagator theory

Electron affinities and electron detachment energies may be calculated by solving the Dyson equation,[17–19] a convenient form of which reads

$$[F + \Sigma(E)]\,\varphi_r = \varepsilon_r \varphi_r. \tag{1}$$

In the latter equation, F is the Fock operator with the usual Coulomb and exchange components that depend on a one-electron density matrix that may be correlated. The self-energy operator, Σ(E), describes the effects of final-state orbital relaxation and differential electron correlation. Because this operator is energy-dependent, self-consistent solutions of the Dyson equation are obtained when E is equal to an electron binding energy, ϵ_r. The eigenfunctions, φ, are proportional to Dyson orbitals, Φ, that are related to many-electron wave functions, Ψ, by the following equations that apply respectively to electron detachment energies and electron affinities of N-electron systems:

$$\Phi_r(x_1) = N^{0.5} \int \Psi_N(x_1, x_2, x_3, \ldots, x_N) \Psi^*_{r,N-1} \times (x_2, x_3, x_4, \ldots, x_N)\, dx_2 dx_3 dx_4 \ldots dx_N, \tag{2}$$

$$\Phi_r(x_1) = (N+1)^{0.5} \int \Psi^*{}_N(x_2, x_3, \ldots, x_{N+1}) \Psi^*_{r,N+1} \times (x_1, x_2, x_3, \ldots, x_{N+1})\, dx_2 dx_3 dx_4 \ldots dx_{N+1}. \tag{3}$$

In the latter equations, x_i represents the space-spin coordinates of electron i. The Dyson orbitals are not necessarily normalized to unity. Their pole strengths, defined by

$$P_r = \int |\Phi_r(x)|^2 dx, \tag{4}$$

may be determined by

$$P_r = \int \phi_r^*(x)\, \Sigma'(E)\, \varphi_r(x)\, dx, \tag{5}$$

where

$$\Sigma'(E) = d\Sigma(E)/dE. \tag{6}$$

In the present calculations, the self-energy matrix is assumed to be diagonal in the canonical, Hartree-Fock orbital basis. Several approximations of this kind have proven successful in determining the lowest electron binding energies of closed-shell molecules. They include the partial third order (P3),[28] P3+,[29] and Outer Valence Green Function (OVGF)[30,31] approximations for the self-energy. Because nondiagonal elements of the self-energy operator are neglected, Dyson orbitals are equal to the square-root of the pole strength times a canonical, Hartree-Fock orbital, ψ^{HF}, i.e.,

$$\Phi_r = P_r^{0.5} \psi_r^{HF}. \tag{7}$$

Vertical electron affinities of CH_3^+ and SiH_3^+ at the optimized geometries of these cations have been calculated with all three self-energy approximations mentioned above. (MP2/cc-pvtz optimizations on the D_{3h} geometries of the cations produce C–H and Si–H bond lengths of 1.079 and 1.461 Å, respectively.) Differences between these electron affinities constitute vertical excitation energies of the corresponding radicals. In the diagonal self-energy approximation, electron binding energies equal the sum of a canonical, Hartree-Fock orbital energy and a diagonal self-energy matrix element. Therefore, it is possible to calculate corrections to the results of Koopmans's theorem for every Hartree-Fock orbital. With increasing Hartree-Fock orbital energies, the relaxation and correlation corrections contained in the self-energy term decrease, pole strengths approach unity and the diagonal self-energy approximation becomes more exact. To describe

the diffuse character of the Rydberg states of the radicals, the cc-pvtz basis was augmented by a 9*s*9*p*9*d*6*f* set of Cartesian gaussian primitive functions on C or Si in which consecutive exponents of a given angular momentum have a constant ratio of one third. The same ratio also relates the least diffuse *s*, *p*, *d*, and *f* functions of the 9*s*9*p*9*d*6*f* set to their most diffuse counterparts in the cc-pvtz set.

All electron propagator calculations were performed with the developers' version of the Gaussian program.[32]

B. Molecular quantum defect orbital method

The MQDO approach has been extensively reported in previous papers,[24,33] thus only the major points are briefly outlined here. In this approach, the radial part of the MQDO wave functions is obtained by analytical solution of a one-electron Schrödinger equation that contains a parametric potential which accounts for electron screening. The angular part of the MQDO wave functions is a linear combination of spherical harmonics, selected in such a way that the complete MQDO's form basis functions for each of the irreducible representation of the molecular symmetry group. This allows the factorization of the electronic transition moment into radial and angular parts, so that the photoionization cross section, in units of megabarns (Mb), adopts the following expression:

$$\sigma = 2.6891 \left[\frac{Z_{net}}{(n-\delta)^2} + k^2 \right] \frac{1}{2k} Q\{a \rightarrow b\} \left| R_{ab} \right|^2, \quad (8)$$

where a and b represent a bound and a continuous state, respectively. Z_{net} is the effective nuclear charge acting on the Rydberg electron. k is the kinetic energy of the free electron upon ionization. δ is the quantum defect which accounts for penetration into the core region. $Q\{a \rightarrow b\}$, referred to as the angular factors, result from the integration of the angular part and R_{ab} from the radial part.

In the central potential model approximation, the expression of the asymmetry parameter for the photoionization of an electron with orbital angular momentum quantum number l is given by[34]

$$\beta = \frac{l(l-1)R_{l-1}^2 + (l+1)(l+2)R_{l+1}^2 - 6l(l+1)R_{l-1}R_{l+1}\cos(\xi_{l+1} - \xi_{l-1})}{(2l+1)\left[lR_{l-1}^2 + (l+1)R_{l+1}^2\right]}, \quad (9)$$

where $R_{l\pm1}$ are the radial dipole matrix elements and $\xi_{l\pm1}$ are the phase shifts of the respective scattered waves. The phase shift ξ_l is presently calculated as a sum of a Coulomb shift and a non-Coulomb shift. The non-Coulomb shift is represented by $\pi\delta_l$ as proposed by Burgess and Seaton[35] for calculations on atomic photoionization magnitudes. The radial transition moments within the MQDO model result in closed-form analytical expressions, which offer, in our view, an important computational advantage.

III. RESULTS AND DISCUSSION

A. Transition energies

The ground state and Rydberg states of CH_3 have both reported to be planar with a D_{3h} geometry.[15] At its equilibrium geometry, the electronic configuration of the X^2A_2'' ground state of the methyl radical is $(1a_1')^2\ (2a_1')^2\ (1e')^4\ (1a_2'')^1$. The ground state of the silyl radical is pyramidal with a configuration $(1a_1)^2\ (2a_1)^2\ (3a_1)^2(1e)^4\ (4a_1)^2\ (2e)^4\ (5a_1)^1\ X^2A_1$ in C_{3v} notation. Calculations of the vertical spectrum of SiH_3 performed by Olbrich[15] with the multi-reference double excitation configuration interaction (MRD-CI) method predict all Rydberg states to be planar, with a D_{3h} geometry. Electron propagator calculations therefore have been performed at the D_{3h} geometry of SiH_3^+.

TABLE I. Vertical electron affinities (for $1a_2''$ only) and excitation energies (eV) for CH_3.

MO	Δ_{KT}	Δ_{P3}	l[a]	MO	Δ_{KT}	Δ_{P3}	l[a]
$1a_2''$	7.77	9.75	1	$3e''$	6.92	8.90	*3*
$3a_1'$	4.23	5.90	0	$6e'$	6.92	8.90	3
$2e'$	5.30	7.14	1	$4a_2''$	6.92	8.90	3
$2a_2''$	5.59	7.36	1	$8a_1'$	6.93	8.88	0
$3e'$	6.11	7.95	2	$7e'$	7.07	9.03	1
$4a_1'$	6.16	8.01	0	$5a_2''$	7.11	9.05	1
$1e''$	6.24	8.17	2	$8e'$	7.18	9.13	2
$5a_1'$	6.26	8.19	0	$9a_1'$	7.20	9.15	2
$4e'$	6.58	8.51	1	$4e''$	7.22	9.19	1
$3a_2''$	6.67	8.58	1	$2a_2'$	7.24	9.21	3
$5e'$	6.84	8.75	2	$10a_1'$	7.24	9.21	3
$6a_1'$	6.87	8.79	0	$5e''$	7.24	9.21	3
$2e''$	6.91	8.87	2	$9e'$	7.24	9.21	3
$1a_2'$	6.92	8.90	3	$6a_2''$	7.24	9.22	3
$7a_1'$	6.92	8.90	3	$11a_1'$	7.23	9.21	0

[a]Angular momentum quantum number of C basis functions with largest coefficients.

Tables I and II display the first vertical electron affinities calculated with Koopmans theorem (KT) results in addition to those obtained with the P3 method. (The OVGF and P3+ methods produce similar results, especially for the most highly excited states.) Excitation energies inferred from differences of electron affinities are listed under columns labelled by Δ. Relatively large discrepancies are seen between the KT and electron-propagator predictions. All pole strengths exceed 0.85 and therefore validate the neglect of off-diagonal elements of the self-energy which occurs in P3 calculations. (Three sets of seven, quasi-degenerate orbitals with Si f character and HF orbital energies of −5.16, −0.85, and −0.55, corresponding respectively to vertical excitation energies of 1.50, 5.81, and 7.19 eV, have been omitted from Table II.) Excitation energies based on the P3 self-energy, which gave the best results of all electron-propagator methods tested, are used in the following sections.

B. Photoionization cross sections and asymmetry parameters

The MQDO approach has been used to calculate the cross-sections for the different continua-accessible Rydberg channels arising from the photoionization of the outermost electron of the ground state of both methyl and silyl radicals. For one-photon transitions, the most intense ones will be those which obey the atomic selection rule $\Delta l = \pm 1$ in addition to the selection rules of molecular symmetry and multiplicity. The requirement $\Delta l = \pm 1$ has long been considered to

TABLE II. Vertical electron affinities (for $2a_2''$ only) and excitation energies (eV) for SiH_3.

MO	Δ_{KT}	Δ_{P3}	l[a]	MO	Δ_{KT}	Δ_{P3}	l[a]
$2a_2''$	6.66	7.86	1	$13e'$	6.36	7.56	2
$5a_1'$	3.62	4.34	0	$8e''$	6.37	7.56	2
$6a_1'$	4.09	4.56	0	$16a_1'$	6.37	7.56	2
$4e'$	4.24	4.96	2	$14e'$	6.40	7.60	2
$4a_2''$	4.70	5.75	1	$17a_1'$	6.40	7.60	0
$5e'$	4.72	5.61	1	$9e''$	6.40	7.60	2
$2e''$	5.01	6.02	2	$15e'$	6.41	7.61	1
$7a_1'$	5.29	6.41	0	$10a_2''$	6.42	7.61	1
$8a_1'$	5.46	6.54	0	$18a_1'$	6.46	7.62	0
$6e'$	5.50	6.61	1	$16e'$	6.47	7.67	2
$7e'$	5.64	6.76	1	$10e''$	6.47	7.67	2
$5a_2''$	5.65	6.80	1	$19a_1'$	6.47	7.66	0
$3e''$	5.74	6.85	2	$11a_2''$	6.48	7.66	1
$10a_1'$	5.89	7.06	2	$17e'$	6.48	7.66	2
$11a_1'$	5.95	7.11	0	$11e''$	6.48	7.67	3
$9e'$	6.27	7.13	2	$20a_1'$	6.49	7.68	0
$10e'$	6.04	7.21	2	$4a_2'$	6.49	7.67	3
$7a_2''$	6.05	7.23	1	$18e'$	6.51	7.71	1
$5e''$	6.08	7.23	2	$12a_2''$	6.51	7.71	1
$13a_1'$	6.19	7.37	0	$21a_1'$	6.52	7.67	0
$14a_1'$	6.20	7.39	0	$22a_1'$	6.56	7.76	0
$11e'$	6.21	7.39	2	$19e'$	6.57	7.77	1
$7e''$	6.26	7.43	2	$13a_2''$	6.57	7.77	1
$12e'$	6.27	7.46	1	$23a_1'$	6.60	7.80	0
$9a_2''$	6.27	7.47	1	$20e'$	6.61	7.81	1
$15a_1'$	6.35	7.55	0	$14a_2''$	6.61	7.81	1

[a]Angular momentum quantum number of Si basis functions with largest coefficients. Some l = 3 states have been omitted (see text).

be much less important than the latter. However, Johnson and Hudgens[6] claim that the Δl rule governs the Rydberg spectra of both methyl and silyl radicals since *l* of the highest occupied orbital in the ground state and of the Rydberg states of CH_3 and SiH_3 are well defined. In both radicals, the outermost occupied molecular orbital in the ground state is comprised mostly of an atomic "*p*" orbital of the central atom. The dipole selection rules together with the selection rules of molecular symmetry, restrict the ionization to the ksa_1', kda_1', and kde'' Rydberg channels for CH_3 and SiH_3 radicals. It is worthwhile noting that Herzberg[12,13] assigned the most intense bands observed in the discrete spectrum of CH_3 to three Rydberg series converging to the first ionization potential. These series correspond to an excitation of an electron from $1a_2''$ to nsa_1', nda_1', and nde'' orbitals.

Calculations of photoionization cross sections with the MQDO method require data of the ionization potential and quantum defects of the s and d Rydberg series. For the ionization energies of the outermost valence orbitals of methyl and silyl radicals, that is $1a_2''$ and $2a_2''$, we have adopted the values of 9.84 eV measured by Houle and Beauchamp[36] and 8.14 eV reported by Johnson and Hudgens,[6] respectively. The quantum defects have been deduced through the well-known Rydberg formula. In the calculations we have used the present vertical excitation energies determined using *ab initio* propagator electron theory.

In Table III we have displayed the MQDO photoionization cross sections versus the incident photon energy up to 50 eV for the Rydberg channels to which the photoionization of the ground state's outermost electron gives rise for methyl and silyl radicals, respectively. The photoionization cross sections leading to the ground states of the cationic cores of both radicals are plotted in Figure 1. These values have been determined by adding the contributions of the three channels.

An inspection of Table III reveals that the kde'' channel represents the main contribution to the partial cross section of methyl radical. This is consistent with the suggestion of Green and Decleva[37] that, in general, the $l \rightarrow l+1$ transition is the dominant contribution. The profile shown in Figure 1 for the methyl radical displays the general behaviour of the cross section with photon energy for molecular orbitals with predominant 2*p* character. That is, the cross section has highest values near the ionization threshold and shows monotonic decreases with increasing photon energy. This decrease can be explained on the basis of the oscillatory nature of continuum orbitals as the kinetic energy of the photoelectron increases. As a consequence, the contributions of opposite sign to the matrix element for photoionization tend to cancel.

The accuracy of the present calculations for methyl radical can be estimated by comparison with experimental results. Data for either electronic state partial photoionization cross-sections or for different Rydberg ionization channels do not appear to be available, but measurements of cross-sections for the absolute photoionization of methyl radical have been reported in the literature at photon energies between 10 and 11 eV. Taking into account that the location of the second electronic state of the methyl cation is at 15.64 eV,[38] it can be assumed that, at the range energy where experimental data are available, the cation is derived primarily from the $1a_2''$ ionization, and hence our calculations can be compared with experimental data. Taatjes *et al.*[2] measured the absolute photoionization cross-sections of the methyl radical at photon energies between 10.2 and 11 eV by using two independent methods. Both techniques use the photolysis of a suitable precursor to produce the methyl radical in conjunction with a species of known cross-section. In one of them, these authors used a pulsed laser-photolysis/time-resolved synchrotron photoionization mass spectrometer whereas in the other, they used a molecular-beam ion-imaging apparatus. Gans *et al.*[8] measured the absolute photoionization cross sections of CH_3 at a photon energy of 10.49 eV by using pyrolysis as source of methyl radicals. Loison[9] measured the absolute photoionization at a photon energy of 10.54 eV by using photodissociation of methane in conjunction with the $CH_3 + NO_2 \rightarrow CH_3O + NO$ reaction in a fast flow reactor. All experimental data are collected in Table IV together with the results obtained in the present work. In order to avoid congestion in Figure 1, we only show some of the experimental data in the figure. As can be seen from Table IV, our results are in good agreement, within the error bars, with the experimental measurements.

As regards the silyl radical, MQDO results predict that the cross section for the kde'' and kda_1' Rydberg channels goes through a minimum, as the photon energy is increased. For atoms, a feature known as the Cooper minimum is observed in the photoionization cross sections from subshells whose

TABLE III. Photoionization cross sections, in units of Mb, for the different Rydberg channels of CH_3 and SiH_3 leading to the ground state of the cationic cores.

	CH_3				SiH_3		
Photon energy (eV)	ksa_1'	kde''	kda_1'	Photon energy (eV)	ksa_1'	kde''	kda_1'
10.0	0.375	2.889	1.897	8.5	0.534	2.987	0.329
10.5	0.326	3.328	2.191	9.0	0.454	2.447	0.238
11.0	0.286	3.672	2.422	9.5	0.390	2.020	0.173
11.5	0.253	3.937	2.601	10.0	0.338	1.681	0.126
12.0	0.224	4.135	2.736	10.5	0.295	1.407	0.091
12.5	0.201	4.278	2.834	11.0	0.259	1.185	0.065
13.0	0.181	4.376	2.902	12.0	0.204	0.854	0.033
14.0	0.148	4.467	2.968	14.0	0.134	0.465	0.006
16.0	0.105	4.386	2.921	16.0	0.093	0.266	0.000
18.0	0.078	4.133	2.758	18.0	0.068	0.158	0.001
20.0	0.060	3.819	2.552	20.0	0.051	0.096	0.003
22.0	0.048	3.497	2.339	22.0	0.040	0.059	0.005
24.0	0.039	3.189	2.136	24.0	0.031	0.036	0.007
26.0	0.032	2.906	1.947	26.0	0.025	0.022	0.009
28.0	0.027	2.648	1.776	28.0	0.021	0.014	0.010
30.0	0.023	2.418	1.622	30.0	0.017	0.008	0.011
32.0	0.020	2.211	1.484	32.0	0.015	0.005	0.012
34.0	0.018	2.027	1.361	34.0	0.012	0.003	0.012
36.0	0.016	1.862	1.251	36.0	0.011	0.001	0.012
38.0	0.014	1.714	1.153	38.0	0.009	0.001	0.012
40.0	0.012	1.582	1.064	40.0	0.008	0.000	0.012
42.0	0.011	1.464	0.985	42.0	0.007	0.000	0.012
44.0	0.010	1.357	0.913	44.0	0.006	0.000	0.012
46.0	0.009	1.261	0.849	46.0	0.005	0.000	0.011
48.0	0.008	1.174	0.791	48.0	0.005	0.000	0.011
50.0	0.008	1.095	0.738	50.0	0.004	0.001	0.011

radial wave functions have nodes; they appear in $l \rightarrow l + 1$ transitions due to a change in sign of the radial dipole matrix element.[39] Carlson *et al.*[40] suggested that Cooper minimum effects would be expected in the photoionization cross sections in molecular orbitals derived from those atomic orbitals that exhibit a Cooper minimum. Since the $2a_2''$ orbital of silyl radical is predominantly a silicon $3p$ orbital, the presence of such minimum in the kd channels is expected. As can be seen in Table III, MQDO results predict Cooper minima at photon energies of about 16 and 44 eV for the kda_1 and kde'' Rydberg channels, respectively. The minimum at around 44 eV is less pronounced than those found in the kda_1 channel, for the cross sections are very small in the energy region where they appear. The photon energy region below 28 eV, were the minimum for the kda_1 channel has been detected, is dominated by the kde'' cross section and therefore no minimum is found in the cross section profile in this energy range. At higher photon energies, no net minimum has been observed in the photoionization cross section profile from the $2a_2''$ orbital of SiH_3, for the kda_1 channel is dominant in this region. An inspection of Figure 1 reveals that the decay of the photoionization cross

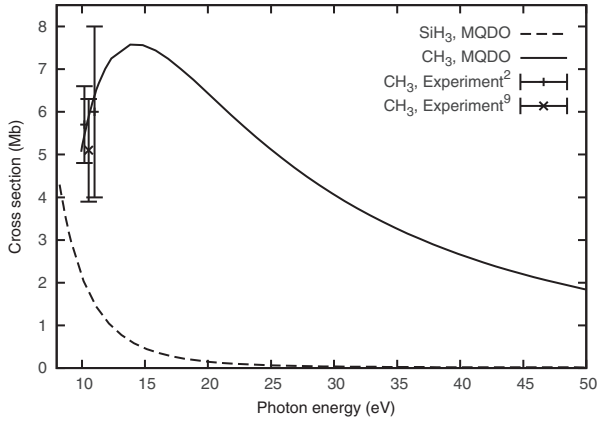

FIG. 1. Cross sections for the photoionization of the outermost orbitals of CH_3 and SiH_3 as a function of photon energy.

TABLE IV. Photoionization cross sections, in units of Mb, of CH_3.

	Cross sections (Mb)	
Photon energy (eV)	Experimental	MQDO[a]
10.2	5.7 ± 0.9[b]	5.45
10.460	5.4 ± 2.0[b]	5.80
10.466	5.5 ± 2.0[b]	5.80
10.471	4.9 ± 2.0[b]	5.81
10.49	$6.7^{+2.4}_{-1.8}$[c]	5.83
10.54	5.1 ± 1.2[d]	5.89
11.0	6.0 ± 2.0[b]	6.38

[a]This work.
[b]Taatjes *et al.*[2]
[c]Gans *et al.*[8]
[d]Loison.[9]

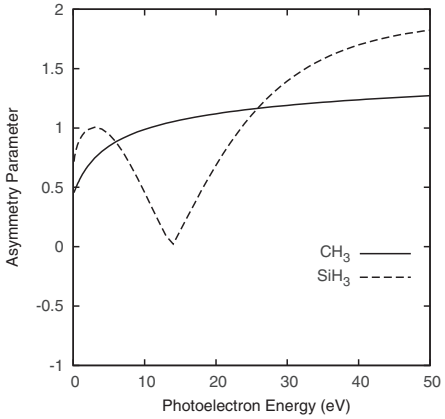

FIG. 2. MQDO asymmetry parameter for the photoionization of the outermost orbital of CH_3 and SiH_3 radicals as a function of photoelectron energy.

section as the photon energy increases is faster for SiH_3 than for CH_3 radical. This behavior is in accord with trends in cross section profiles of the first and second row hydrides observed by Stener and Decleva[41] and, therefore, could be taken as an indication of the correctness of MQDO results given that no comparative data seem to be available.

It is to be noted that even when the Cooper minima do not significantly affect the cross sections, they have a noteworthy effect on the asymmetry parameters.[42] So, in order to confirm the presence of a Cooper minimum in the photoionization of the outermost electron of SiH_3, we have calculated the asymmetry parameter β over the 0–40 eV photoelectron energy range. The results are shown in Figure 2. The Cooper minimum appears at photoelectron energy of about 14 eV, which corresponds to a photon energy of 22 eV. Unfortunately neither experimental nor theoretical data have been reported yet for the photoelectron angular distribution of silyl radical. Thus it could be of interest to compare the present β profile to the behavior exhibited by a p subshell having a Cooper minimum. For that matter, the general trend for the asymmetry parameter from ionization of a $3p$ orbital is an increase in β above the threshold, followed by a decrease to a minimum and then an asymptotically increasing behavior.[41] This behavior is exhibited by the MQDO data for SiH_3, which gives us confidence in their reliability.

We have also calculated the distribution angular profile for the outermost orbital of methyl radical. The MQDO results are plotted in Figure 2. The general shape of the asymmetry parameter for methyl radical is quite different from that of silyl radical. The β parameter has no Cooper minimum since the $1a_2''$ orbital is mainly an atomic $2p$ orbital and, thus, nodeless. Given that no comparative data have been found for the asymmetry parameter in CH_3 radical, as an indicator of the correctness of the present results, we use the general behavior of the angular distributions of photoelectrons for a p subshell having no Cooper minimum. That is, the asymmetry parameter shows a quite rapid increase with the increasing photoelectron energy followed by flat behavior at high photoelectron energy. Inspection of Figure 2 shows that the MQDO β profile for the $1a_2''$ orbital of CH_3 shows the general shape of the asymmetry parameter for a p subshell having no Cooper minimum, which may reveal the correctness of the present calculations, at least at a qualitative level.

IV. CONCLUSIONS

In the present work, vertical excitation energies pertaining to Rydberg states of CH_3 and SiH_3 radicals have been inferred from electron propagator calculations of the vertical electron affinities of the corresponding cations. The latter calculations have employed large sets of diffuse functions and several self-energy approximations.

Cross section and asymmetry parameter profiles for the photoionization of the outermost orbital of methyl and silyl radicals are reported, as far as we know, for the first time. In addition, contributions of the various continuum channels to the photoionization cross section have been analyzed. According to the MQDO calculations, a Cooper minimum has been found in the kde″ and kda_1' Rydberg channels of SiH_3, although a minimum in the electronic partial cross section profile is not observed. However, our results for the asymmetry parameter show the presence of a Cooper minimum in the photoionization of this radical. Concerning the CH_3 radical, the MQDO results for photoionization cross sections agree quite well with the scarce experimental data available.

Overall, we are confident in the potential usefulness of the excitation energies and photoionization parameters of CH_3 and SiH_3 in the present work, as well as in the adequacy of our theoretical methods for dealing with spectroscopic properties of molecular radicals. We also hope that this work stimulates further investigations on the appearance of a Cooper minimum in the photoionization of silyl radical.

ACKNOWLEDGMENTS

This work has been supported by the Spanish Ministerio de Ciencia e Innovación (MICINN) (Project No. CTQ2010-17892) and the Junta de Castilla y León (Project No. VA077U13). Part of this work was completed with the support of a grant (CHE-0809199) to Auburn University by the National Science Foundation.

[1] E. Hirota, Pure Appl. Chem. **70**, 1145 (1998).
[2] C. A. Taatjes, D. L. Osborn, T. M. Selby, G. Meloni, H. Fan, and S. T. Pratt, J. Phys. Chem. A **112**, 9336 (2008).
[3] H. Feuchtgruber, F. P. Helmich, E. F. van Dishoek, and C. M. Wright, Astrophys. J. **535**, L111 (2000).
[4] B. Bézard, H. Feuchtgruber, J. I. Moses, and T. Encrenaz, Astron. Astrophys. **334**, L41–L44 (1998).
[5] B. Bézard, P. Romani, H. Feuchtgruber, and T. Encrenaz, Astrophys. J. **515**, 868 (1999).
[6] R. D. Johnson III and J. W. Hudgens, J. Chem. Phys. **94**, 5331 (1991).
[7] J. M. Jasinski, B. S. Meyerson, and B. A. Scott, Annu. Rev. Phys. Chem. **38**, 109 (1987).
[8] B. Gans, L. A. Vieira Mendes, S. Boyé-Péronne, S. Douin, G. Garcia, H. Soldi-Lose, B. K. Cunha de Miranda, C. Alcaraz, N. Carrasco, P. Pernot, and D. Gauyacq, J. Phys. Chem. A **114**, 3237 (2010).
[9] J.-C. Loison, J. Phys. Chem. A **114**, 6515 (2010).
[10] J. Berkowitz, Radiat. Phys. Chem. **32**, 23 (1988).
[11] A. V. Baklanov and L. N. Krasnoperov, J. Phys. Chem. A **105**, 4917 (2001).
[12] G. Herzberg, Proc. R. Soc. London, Ser. A **262**, 291 (1961).
[13] G. Herzberg, *Molecular Spectra and Molecular Structure. III. Electronic Spectra and Electronic Structure of Polyatomic Molecules*, reprint edition (Krieger, Florida, 1991), pp. 513–609.

[14]R. D. Johnson III and J. W. Hudgens, Chem. Phys. Lett. **141**, 163 (1987).
[15]G. Olbrich, Chem. Phys. **101**, 381 (1986).
[16]R. D. Johnson III, B. P. Tsai, and J. W. Hudgens, J. Chem. Phys. **91**, 3340 (1989).
[17]J. V. Ortiz, WIREs Comput. Mol. Sci. **3**, 123 (2013).
[18]V. G. Zakrzewski, O. Dolgounitcheva, A. V. Zakjevskii, and J. V. Ortiz, Adv. Quantum Chem. **62**, 105 (2011).
[19]V. G. Zakrzewski, O. Dolgounitcheva, A. V. Zakjevskii, and J. V. Ortiz, Ann. Rev. Comput. Chem. **6**, 79 (2010).
[20]J. W. Gallagher, C. E. Brion, J. A. R. Samson, and P. W. Langhoff, J. Phys. Chem. Ref. Data **17**, 9 (1988).
[21]A. M. Velasco, I. Martín, and C. Lavín, Chem. Phys. Lett. **264**, 579 (1997).
[22]I. Martín, A. M. Velasco, and C. Lavín, Int. J. Quantum Chem. **86**, 59 (2002).
[23]E. Bustos, A. M. Velasco, I. Martín, and C. Lavín, J. Phys. Chem. A **108**, 1923 (2004).
[24]C. Lavín, A. M. Velasco, and I. Martín, Astrophys. J. **692**, 1354 (2009).
[25]A. M. Velasco, C. Lavín, I. Martín, J. Melin, and J. V. Ortiz, J. Chem. Phys. **131**, 024104 (2009).
[26]M. V. Vega, C. Lavín, and A. M. Velasco, J. Chem. Phys. **136**, 214308 (2012).
[27]C. Lavín, M. V. Veja, and A. M. Velasco, J. Phys. Chem. A **116**, 11913 (2012).
[28]J. V. Ortiz, J. Chem. Phys. **104**, 7599 (1996).
[29]J. V. Ortiz, Int. J. Quantum Chem. **105**, 803 (2005).
[30]W. von Niessen, J. Schirmer, and L. S. Cederbaum, Comput. Phys. Rep. **1**, 57 (1984).
[31]V. G. Zakrzewski, J. V. Ortiz, J. A. Nichols, D. Heryadi, D. L. Yeager, and J. T. Golab, Int. J. Quantum Chem. **60**, 29 (1996).
[32]M. J. Frisch, G. W. Trucks, H. B. Schlegel *et al.*, GAUSSIAN 08, Developers′ version, Revision H.01, Gaussian, Inc., Wallingford, CT, 2008.
[33]I. Martín, C. Lavín, A. M. Velasco, M. O. Martín, J. Karwowski, and G. H. F. Diercksen, Chem. Phys. **202**, 307 (1996).
[34]J. Cooper and R. N. Zare, "Photoelectron angular distribution," in *Lectures in Theoretical Physics: Atomic Collision Processes*, edited by S. Geltman, K. T. Mahanthappa, and W. E. Brittin (Gordon and Breach, New York, 1969), Vol. 11C, p. 322.
[35]A. Burges and M. J. Seaton, Mon. Not. R. Astron. Soc. **120**, 121 (1960).
[36]F. A. Houle and J. L. Beauchamp, J. Am. Chem. Soc. **101**, 4067 (1979).
[37]J. C. Green and P. Decleva, Coord. Chem. Rev. **249**, 209 (2005).
[38]H. M. Rosenstock, K. Draxl, B. W. Steiner, and J. T. Herron, "Ion Energetics Data," *NIST Chemistry WebBook, NIST Standard Reference Database Number 69*, Eds. P. J. Linstrom and W. G. Mallard, National Institute of Standards and Technology, Gaithersburg MD, 20899, see http://webbook.nist.gov.
[39]J. W. Cooper, Phys. Rev. **128**, 681 (1962).
[40]T. A. Carlson, M. O. Krause, W. A. Svensson, P. Gerard, F. A. Grimm, T. A. Whithley, and B. P. Pullen, Z. Phys. D: At., Mol. Clusters **2**, 309 (1986).
[41]M. Stener and P. Decleva, J. Electron Spectrosc. Relat. Phenom. **94**, 195 (1998).
[42]S. T. Manson, A. Msezane, A. F. Starace, and S. Shahabi, Phys. Rev. A **20**, 1005 (1979).